Journal of Applied Electrochemistry **33**: 1025–1033, 2003.

A thermodynamic approach to calculate the yttria-stabilized zirconia pH sensor potential

W. ZHANG and E.A. CHARLES*
Corrosion Research Centre, University of Newcastle upon Tyne, NE1 7RU, Great Britain
*(*author for correspondence, e-mail: e.a.charles@newcastle.ac.uk)*

Received 3 May 2002; accepted in revised form 20 May 2002

Key words: high temperature pH, primary pH sensor, yttria-stabilized zirconia (YSZ) sensor

Abstract

Published thermodynamic approaches to calculate the yttria-stabilized zirconia (YSZ) ceramic pH sensor potential are reviewed. A thermodynamic approach related to the Gibbs free energies of reactants and products is proposed to calculate the YSZ pH sensor potential, identify the YSZ pH sensors as primary pH sensors and to determine solution pH at high temperatures. YSZ thimbles have been used with a silver powder internal element prepared in the presence of dry air to generate a redox system, $Ag|O_2$, sensitive to pH. YSZ ($Ag|O_2$) pH sensors have been tested over a temperature range of 100 to 300 °C in lithiated boric acid solutions which are related to pressurized water reactor coolant chemistry. The test results have good agreement with the thermodynamic calculation from 100 to 300 °C. The thermodynamic calculation can be applied to a variety of YSZ pH sensor internal elements including $Cu|Cu_2O$, $Hg|HgO$, $Ag|Ag_2O$, $Ag|O_2$, whereas earlier published calculations are not generally applicable.

List of symbols

a_{H_2O}	activity of water
a_{H_2}	activity of dissolved molecular hydrogen
a_{H^+}	activity of hydrogen ion
$E^\circ_{O_2/H_2O}$	standard potential of oxygen–water reaction half cell
$E^\circ_{H_2/O_2}$	standard potential of the hydrogen–oxygen–water reaction
E°_{M/M_xO_y}	standard potential of metal/metal oxide internal element
E_{Pt/H_2}	hydrogen (platinum) electrode (H_2(Pt)) half cell potential
E_{ref}	reference electrode half cell potential
E_Y	YSZ pH sensor half cell potential
f_{H_2}	fugacity of dissolved molecular hydrogen
K_H	Henry's law constant
$\Delta G^\circ_{metal/metal\ oxide}$	standard Gibbs free energies of formation of oxides
m_{H_2}	mole fraction of the solute hydrogen in the liquid phase
p_{O_2}	oxygen partial pressure

Greek symbols

γ_{H_2}	activity coefficient of the solute hydrogen in the liquid phase
$\mu^\circ_{e^-}$	standard partial molar Gibbs free energy of an electron
$\mu^\circ_{H_2O}$	standard partial molar Gibbs free energy of H_2O
$\mu^\circ_{H^+}$	standard partial molar Gibbs free energy of H^+
$\mu^\circ_{O_2}$	standard partial molar Gibbs free energy of O_2

1. Introduction

Real time measurement of *in situ* pH in high temperature and high-pressure aqueous systems has been a major challenge for remote control of industrial processes, including power station and chemical plant installations. Monitoring of pH can help to optimize water chemistry conditions for plant and keep corrosion to a minimum. High temperature pH measurements also allow the direct evaluation of thermodynamic and solution chemistry theories and the acquisition of data for the thermodynamic database. With the advent of the yttria-stabilized zirconia (YSZ) ceramic pH sensor, it is possible to measure the pH of aqueous systems at temperatures as high as 528 °C, even in the presence of redox species [1–5]. The YSZ electrode is most likely to be thermodynamically viable as a primary pH sensor [2–15]. A primary pH sensor does not need to be calibrated using standard pH buffers, and the pH of a solution can be calculated directly from the measured potential using a thermodynamic approach. Although several metal/metal oxide internal elements have been tested [2–15],

one better than the Hg|HgO internal element has not been reported. Mercury is toxic and harmful to the environment if a leak should occur. The YSZ ($Ag|Ag_2O$) pH sensor has a good pH response, but concern about Ag_2O undergoing gradual thermal decomposition to silver metal [4–7] impeded research and the existing thermodynamic calculation can only estimate the YSZ ($Ag|Ag_2O)|H_2$(Pt) whole cell potential within a narrow temperature range [12]. A modified thermodynamic calculation for the YSZ pH sensor potential needs to be developed, if a better thermodynamic analysis of experimental data over a wide range of internal elements and test temperatures is to be achieved.

Niedrach [2, 3] first presented the mechanism of a $Cu|Cu_2O$ YSZ sensor. He measured the conductivity of the YSZ membrane and calculated the activation energy of the sensor, to ascertain that the sensor mechanism involves oxygen ion conduction. He related the measured potential of the YSZ ($Cu|Cu_2O$) sensor to the standard hydrogen electrode scale (SHE) through a thermodynamic calculation based on Reaction 1:

$$Cu_2O + 2\,H^+ + 2\,e^- = 2\,Cu + H_2O \tag{1}$$

Macdonald et al. [4] extended the thermodynamic calculation to several metal/metal oxide internal elements. According to Macdonald et al., the potential difference between YSZ sensor potential (E_Y) and reference electrode potential (E_{ref}, SHE) is given by:

$$E_Y - E_{ref} = E^\circ_{M/M_xO_y} - \frac{RT}{2F}\ln(a_{H_2O}) - \frac{2.303\,RT}{F}\mathrm{pH} \tag{2}$$

Where a_{H_2O} is the thermodynamic activity of water, $pH = -\log(a_{H^+})$, and E°_{M/M_xO_y} is the standard potential of the internal element, which is related to the change in standard chemical potential, $\Delta\mu^\circ_R$, for Reaction 3:

$$(1/y)M_xO_y + H_2 = (x/y)M + H_2O \tag{3}$$

From Equation 2, if we know a_{H_2O} and E°_{M/M_xO_y}, $E_Y - E_{ref}$ (SHE) can be measured and then the pH can be calculated from

$$\mathrm{pH} = \frac{F}{2.303\,RT}(E^\circ_{M/M_xO_y} - E_Y + E_{ref}) - \frac{1}{2}\log(a_{H_2O}) \tag{4}$$

An effective way of establishing the thermodynamic viability of the YSZ sensor is to compare the measured potentials directly with a primary H_2 electrode. In this way the reference electrode potential term (E_{ref}) is eliminated and the measured cell potential is independent of pH. A whole cell potential expression for the YSZ pH sensor against a hydrogen electrode (H_2(Pt)) is given by

$$\Delta E = E_Y - E_{Pt/H_2} = E^\circ_{M/M_xO_y} + \frac{2.303\,RT}{2F}\log\left(\frac{f_{H_2}}{a_{H_2O}}\right) \tag{5}$$

The significance of Equation 5 is that it offers a method by which to determine whether a YSZ electrode is a primary pH electrode. However, the value of E°_{M/M_xO_y} is not always available, for example in the case of Ag_2O decomposing to Ag at temperatures higher than 200 °C.

Danielson et al. [12] analysed the YSZ ($Ag|O_2)|H_2$ (Pt) whole cell potential based on Reaction 6:

$$H_2\ (\text{dissolved}) + 1/2\,O_2(\text{gas-inside}) = H_2O + 2\,e^-(Pt) - 2\,e^-\ (\text{metal}/ZrO_2) \tag{6}$$

Oxygen in the air was assumed to control the oxygen fugacity inside the zirconia sensor tube and dissolved hydrogen in solution was assumed to control the hydrogen fugacity in the autoclave. The potentials of the YSZ ($Ag|O_2)|H_2$ (Pt) cell were calculated from 100 to 300 °C, but they did not derive the equilibrium expression. Macdonald et al. [1] reported the calculation according to the following expression:

$$\Delta E = E^\circ_{H_2/O_2} + \frac{RT}{4F}\ln 0.2 + \frac{2.303\,RT}{2F}\log\left(\frac{f_{H_2}}{a_{H_2O}}\right) \tag{7}$$

where $E^\circ_{H_2/O_2}$ is the theoretical potential for the hydrogen–oxygen electrode under standard conditions based on the reaction described in Equation 6. The approach used by Danielson et al. and Macdonald et al. does not give a method for the correction of the oxygen partial pressure with temperature inside the YSZ tube. Their Equation can only be used to calculate the YSZ ($Ag|O_2)|H_2$ (Pt) whole cell potential within a narrow temperature range and cannot be extended to calculate the potentials of YSZ sensors with other internal elements.

2. Proposed thermodynamic calculation

Because the internal metal/metal oxide elements are separated from the test solution by the YSZ tube, they do not directly react with the solution. The oxygen ion is the conductive element through the YSZ ceramic and it can be envisaged that the function of the internal metal/metal oxide couple is the determination of the oxygen partial pressure inside the YSZ tube and the transformation of oxygen molecules to oxygen ions. In the thermodynamic analysis, the metal/metal oxide reaction inside the YSZ tube can be treated as an intermediate step, represented as

$$O_2 + 4\ e^- = 2\ O^{2-} \tag{8}$$

If the metal/metal oxide reaction is at equilibrium then the chemical potential (the molar Gibbs free energy) of O^{2-}, $\mu_{O^{2-}}$, is determined by the equilibrium O_2 partial pressure for the metal/metal oxide reaction in the tube. If oxygen is deficient inside the tube, $\mu_{O^{2-}}$ is dependent on the O_2 partial pressure in the tube. The

equilibrium O_2 partial pressure of the metal/metal oxide can be calculated from the standard Gibbs free energies of formation of oxides [16]:

$$\Delta G^{\circ}_{\text{metal/metal oxide}} = RT\ln(p_{O_2}) \tag{9}$$

The reaction on the YSZ tube outer surface can be represented by Equations 10 and 11:

$$O^{2-} + H^{+} = OH^{-} \tag{10}$$

$$OH^{-} + H^{+} = H_2O \tag{11}$$

At equilibrium, the net O^{2-} diffusion through the YSZ tube is zero, then summing the interface reactions inside and outside gives the net reaction:

$$O_2 + 4H^{+} + 4e^{-} = 2H_2O \tag{12}$$

At equilibrium, according to the Nernst Equation, the half-cell potential of YSZ electrode can be expressed as

$$\begin{aligned} E_Y &= E^{\circ}_{O_2/H_2O} + \frac{RT}{4F}\ln\left(\frac{p_{O_2}\,a^4_{H^+}}{a^2_{H_2O}}\right) \\ &= E^{\circ}_{O_2/H_2O} + \frac{RT}{4F}\ln(p_{O_2}) - \frac{RT}{2F}\ln(a_{H_2O}) - \frac{2.303\,RT}{F}\text{pH} \end{aligned} \tag{13}$$

and $E^{\circ}_{O_2/H_2O}$ can be derived using

$$E^{\circ}_{O_2/H_2O} = -\frac{\Delta G^{\circ}}{nF} = -\frac{2\mu^{\circ}_{H_2O} - \mu^{\circ}_{O_2} - 4\mu^{\circ}_{H^+} - 4\mu^{\circ}_{e^-}}{4F} \tag{14}$$

where, $\mu^{\circ}_{H_2O}$, $\mu^{\circ}_{O_2}$ and $\mu^{\circ}_{H^+}$ are the standard partial molar Gibbs free energies. Now $\mu^{\circ}_{H^+}$ is assigned to zero at all temperatures and pressures in the thermodynamic database. Table 1 lists values of $\mu^{\circ}_{H_2O}$ and $\mu^{\circ}_{O_2}$ obtained from [17]. The term $\mu^{\circ}_{e^-}$ is the standard partial molar Gibbs free energy (escape tendency) of an electron. In solid state physics, $\mu_{e^-} = \varepsilon_F N_A$, where ε_F is Fermi level and N_A is Avogadro's number [18]. In electrochemistry, when electrodes are in contact with solutions, their Fermi levels change, and there will be a potential difference between the electrode and the solution, this potential difference is a half-cell potential. The half-cell potentials of electrodes can be related to SHE scale. For the hydrogen electrode, H_2(Pt), when the activities of hydrogen and hydrogen ion are unity, Equation 15 can be derived:

$$2\mu^{\circ}_{H^+} + 2\mu^{\circ}_{e^-} = \mu^{\circ}_{H_2} \tag{15}$$

Because $\mu^{\circ}_{H^+}$ is assigned to zero at all temperatures and pressures in the thermodynamic database then, at any temperature and pressure,

$$\mu^{\circ}_{e^-} = \frac{1}{2}\mu^{\circ}_{H_2} \tag{16}$$

where $\mu^{\circ}_{H_2}$ is the standard partial molar Gibbs free energy of formation of H_2 which is listed in Table 1 [17]. The significance of Equation 16 is that it is now possible to relate the half-cell potential of an electrode at any temperature to the SHE by thermodynamic calculation. At 25 °C, $\mu^{\circ}_{e^-}$ is assigned to zero by the definition of the SHE scale, $\mu^{\circ}_{H_2}$ at 25 °C is also assigned to zero in the thermodynamic database. At temperatures other than 25 °C, Equation 16 can be used to calculate the change of $\mu^{\circ}_{e^-}$ with temperature related to the arbitrary zero at 25 °C (SHE). Equation 14 can be simplified to

$$E^{\circ}_{O_2/H_2O} = -\frac{2\mu^{\circ}_{H_2O} - \mu^{\circ}_{O_2} - 2\mu^{\circ}_{H_2}}{4F} \tag{17}$$

Hence in Equation 13, $E^{\circ}_{O_2/H_2O}$ can be calculated, while E_Y can be measured provided that we have a reference electrode whose potential can be related to SHE. From measured E_Y, pH can be calculated. Thus,

$$\begin{aligned} \text{pH} = {} & \frac{F}{2.303RT}(E^{\circ}_{O_2/H_2O} - E_Y) + \frac{1}{4}\log(p_{O_2}) \\ & - \frac{1}{2}\log(a_{H_2O}) \end{aligned} \tag{18}$$

The measured pH can be compared with the predicted pH from solution chemistry theory.

The reaction on the H_2 (Pt) electrode surface can be represented as

$$2\,H^{+} + 2\,e^{-} = H_2 \tag{19}$$

At equilibrium, the half-cell potential of the H_2 (Pt) electrode can be derived from the following expression:

$$\begin{aligned} E_{Pt/H_2} &= E^{\circ}_{H^+/H_2} + \frac{2.303\,RT}{2F}\log\left(\frac{a^2_{H^+}}{a_{H_2}}\right) \\ &= E^{\circ}_{H^+/H_2} - \frac{2.303\,RT}{2F}\log(a_{H_2}) - \frac{2.303\,RT}{F}\text{pH} \end{aligned} \tag{20}$$

Table 1. Calculated standard partial molar Gibbs free energies of formation for H_2O, O_2 and H_2 as a function of temperature, derived from [17]

Temperature /°C	$\mu^{\circ}_{H_2O}$ (sat. pressure) /kJ mol^{-1}	$\mu^{\circ}_{O_2}$ /kJ mol^{-1}	$\mu^{\circ}_{H_2}$ /kJ mol^{-1}
25	−237.19	0.00	0.00
50	−238.99	−5.15	−3.31
75	−240.96	−10.38	−6.65
100	−243.09	−15.69	−10.04
125	−245.31	−20.96	−13.51
150	−247.65	−26.32	−16.99
175	−250.12	−31.76	−20.54
200	−252.67	−37.20	−24.14
225	−255.35	−42.72	−27.74
250	−258.11	−48.24	−31.38
300	−263.88	−59.41	−38.83
350	−269.99	−70.75	−46.36

where a_{H_2} is the activity of dissolved molecular hydrogen in the test solution and is equal to the hydrogen fugacity (f_{H_2}). $E^{\circ}_{H^+/H_2}$ is always zero Thus,

$$E^{\circ}_{H^+/H2} = -\frac{\Delta G^{\circ}}{nF} = -\frac{\mu^{\circ}_{H_2} - 2\mu^{\circ}_{H^+} - 2\mu^{\circ}_{e^-}}{2F} = 0 \qquad (21)$$

Then, by combining Equations 13, 17, 20 and 21, the whole cell potential of the YSZ pH sensor versus the H_2 (Pt) electrode can be expressed as

$$\begin{aligned}\Delta E &= E_Y - E_{Pt/H_2} \\ &= (E^{\circ}_{O_2/H_2O} - E^{\circ}_{H^+/H_2}) + \frac{RT}{4F}\ln(p_{O_2}) \\ &\quad + \frac{2.303\,RT}{2F}\log(a_{H_2}) - \frac{RT}{2F}\ln(a_{H_2O}) \\ &= -\frac{2\mu^{\circ}_{H_2O} - \mu^{\circ}_{O_2} - 2\mu^{\circ}_{H_2}}{4F} + \frac{RT}{4F}\ln(p_{O_2}) \\ &\quad + \frac{2.303\,RT}{2F}\log\left(\frac{f_{H_2}}{a_{H_2O}}\right) \end{aligned} \qquad (22)$$

where, $-(2\mu^{\circ}_{H_2O} - \mu^{\circ}_{O_2} - 2\mu^{\circ}_{H_2})/4F$ can be calculated from the data that are listed in Table 1 and $RT/4F\ln(P_{O_2})$ can be calculated from Equation 9.

Comparing Equation 22 with Equation 5, E°_{M/M_xO_y} in Equation 5 is replaced by $-((2\mu^{\circ}_{H_2O} - \mu^{\circ}_{O_2} - 2\mu^{\circ}_{H_2})/4F) + (RT/4F)\ln(P_{O_2})$ in Equation 22. The significance of this change is that a thermodynamic analysis of experimental data for a wider range of internal elements and test temperatures can be made, because when the value of E°_{M/M_xO_y} is not available (for example, in the case of Ag_2O decomposing to Ag at high temperatures) the value of $-((2\mu^{\circ}_{H_2O} - \mu^{\circ}_{O_2} - 2\mu^{\circ}_{H_2})/4F) + (RT/4F)\times \ln(P_{O_2})$ can still be found. Comparing Equation 22 with Equation 7, $E^{\circ}_{H_2/O_2} + (RT/4F)\ln 0.2$ in Equation 7 is replaced by $-((2\mu^{\circ}_{H_2O} - \mu^{\circ}_{O_2} - 2\mu^{\circ}_{H_2})/4F) + (RT4F)\times \ln(P_{O_2})$ in Equation 22. The oxygen partial pressure inside the YSZ tube is the dominant factor in generation of the electrode potential thus the change in partial pressure with temperature needs to be accounted for when determining the potential. For the YSZ ($Ag|Ag_2O$) electrode, the equilibrium oxygen partial pressure is higher than 1 atm when the temperature is above 200 °C but such an oxygen partial pressure is not achieved when only small amounts of Ag_2O are placed into the YSZ tube space. When the oxygen partial pressure is lower than the equilibrium oxygen partial pressure then the Ag_2O starts to decompose and the electrode can be better represented as YSZ ($Ag|O_2$) because of its sensitivity to the oxygen partial pressure.

For the YSZ ($Ag|O_2$) electrode, prepared by packing silver powder into a YSZ tube under air, to operate at temperatures below 200 °C, it first needs to be conditioned at higher temperatures to get it to an equilibrium state. When the temperature is higher than 200 °C, the partial pressure of oxygen inside the YSZ tube is lower than the equilibrium oxygen partial pressure and the amount of Ag_2O is negligible. The ideal gas equation can then be used to calculate the oxygen partial pressure inside the YSZ tube. It is known that $P \approx 0.2$ at 25 °C, then at temperatures higher than 200 °C, the oxygen partial pressure can be calculated:

$$P_{O_2} \approx \frac{0.2}{298.15}T \qquad (23)$$

The activity of dissolved molecular hydrogen in the test solution (a_{H_2}), is equal to the hydrogen fugacity (f_{H_2}) and can be calculated:

$$a_{H_2} = f_{H_2} = K_H m_{H_2}\gamma_{H_2} \qquad (24)$$

where K_H is Henry's law constant, m_{H_2} is the mole fraction of the solute hydrogen in the liquid phase and γ_{H_2} is the activity coefficient of the solute hydrogen in the liquid phase. If an autoclave with a recirculating flow test loop operates in a single liquid phase mode, the mole fraction of the solute hydrogen, m_{H_2}, can be considered as almost constant at all points in the loop. Thus, at test temperature, $m_{H_2} \approx m^{\circ}_{H_2}$, hence

$$m_{H_2} = \frac{f_{H_2}}{K_H\gamma_{H_2}} \approx m^{\circ}_{H_2} = \frac{f^{\circ}_{H_2}}{K^{\circ}_H\gamma^{\circ}_{H_2}} \qquad (25)$$

$$a_{H_2} = f_{H_2} = \left[\frac{K_H}{K^{\circ}_H}\right]\left[\frac{\gamma_{H_2}}{\gamma^{\circ}_{H_2}}\right]f^{\circ}_{H_2} \qquad (26)$$

where, at 25 °C, the fugacity of hydrogen is $f^{\circ}_{H_2}$, the mole fraction of the solute hydrogen is $m^{\circ}_{H_2}$, Henry's law constant is K°_H and the activity coefficient of the solute hydrogen is $\gamma^{\circ}_{H_2}$.

From the measured potential (E_{Pt/H_2}) of a hydrogen electrode and using Equations 20, 21 and 26, pH can be calculated from

$$\mathrm{pH} = \frac{F}{2.303\,RT}(-E_{Pt/H_2}) - \frac{1}{2}\log\left(\left[\frac{K_H}{K^{\circ}_H}\right]\left[\frac{\gamma_{H_2}}{\gamma^{\circ}_{H_2}}\right]f^{\circ}_{H_2}\right) \qquad (27)$$

Substitution of Equation 26 into Equation 22 yields:

$$\begin{aligned}\Delta E &= E_Y - E_{Pt/H_2} \\ &= -\frac{2\mu^{\circ}_{H_2O} - \mu^{\circ}_{O_2} - 2\mu^{\circ}_{H_2}}{4F} + \frac{RT}{4F} \\ &\quad \times \ln(P_{O_2}) \\ &\quad + \frac{2.303\,RT}{2F}\log\left(\left[\frac{K_H}{K^{\circ}_H}\right]\left[\frac{\gamma_{H2}}{\gamma^{\circ}_{H_2}}\right]\left[\frac{f^{\circ}_{H_2}}{a_{H_2O}}\right]\right) \end{aligned} \qquad (28)$$

which enables the hydrogen fugacity to be calculated at high temperatures.

3. Experimental details

3.1. *Electrode system and refreshed autoclave*

The electrode system used in this work consisted of an external Ag/AgCl, 0.1 M KCl reference electrode, one or

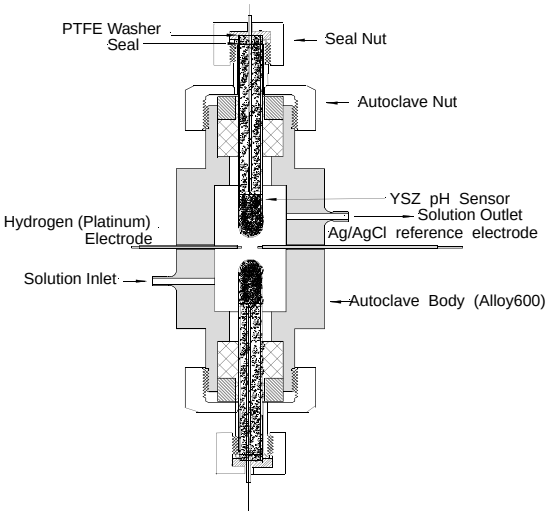

Fig. 1. Cross-section of refreshed autoclave showing the electrode locations.

two pH sensitive YSZ sensors and a platinum electrode. Silver powder was packed into the end of two kinds of YSZ thimbles (about 150 mm long, 9.5 mm outer diameter and 1 mm wall thickness) with and without glass phase to construct the sensors. The sensors were prepared in a dry air glove box to avoid water contamination, a silver wire was embedded in the silver powder to make electrical contact and the sensors were sealed with an epoxy resin after being back filled with inert zirconia sand. The electrodes were fitted into a refreshed autoclave (Inconel-600), which is shown schematically in Figure 1. The solution was held in a reservoir vessel and was purged with H_2 gas at room temperature before entry into the autoclave through a re-circulating loop pressurized to 14 MPa. The YSZ sensors were fitted through PTFE sleeves and Viton O-ring compression seals were used between the autoclave and YSZ sensors. It was found that electrodes had to be conditioned at high temperature prior to use at temperatures below 200 °C to achieve reproducible data.

3.2. *Test solutions*

Solutions were prepared by dissolving 'Analar Reagent' chemicals in distilled and deionized water. Orthoboric acid, monohydrate lithium hydroxide, potassium hydroxide and potassium chloride were used to prepare the electrolytes and their room temperature pH was checked prior to use.

3.3. *Procedure*

All potentials were continuously monitored over time and measurements were taken until the electrode potentials reached equilibrium values. Measurements were made using high input impedance, 10^{12} Ω, buffers which were connected to a differential multiplexor, then fed to a computer for processing. Tests were performed over the temperature range 100–300 °C.

4. Material characterization of YSZ thimbles

The microstructure of the YSZ thimbles was examined prior to electrical characterization. Typical scanning electron microscope (SEM) images for two kinds of YSZ thimbles are shown in Figures 2 and 3, the SEM images of the cross-section of the thimbles showed that there were micropores in the bulk of the materials that arose from the method of the thimble manufacture. The micropores in both materials were distinct and do not produce a connected pore path through the membrane, so the ceramic is a dense membrane. Dark glassy phases at grain boundaries had only been observed on the cross-section surface of one kind of YSZ thimbles, type A (Figure 2); there is no glassy phase visible on the cross-section surface of YSZ thimbles, type B, (Figure 3). Energy dispersive analysis of X-rays (EDX) spot

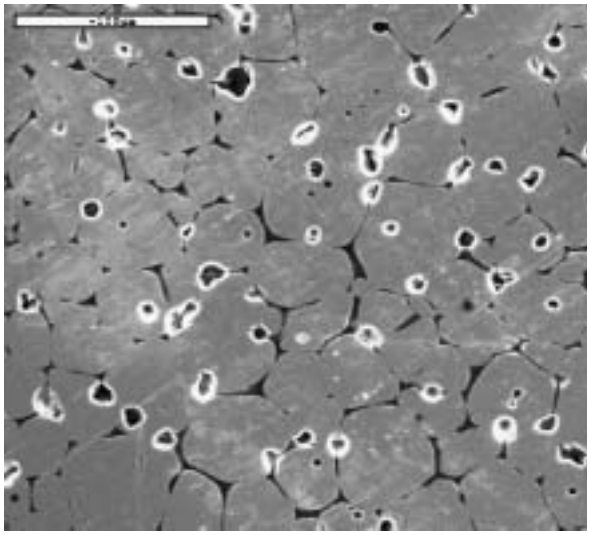

Fig. 2. SEM image of type A YSZ thimble showing glassy phase (black), X400.

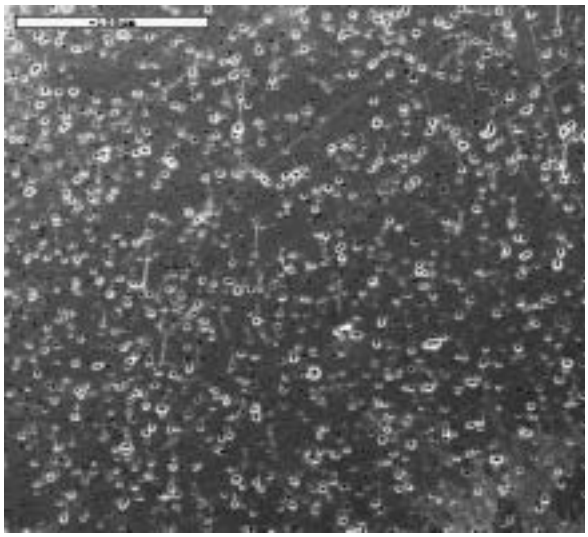

Fig. 3. SEM image of type B YSZ thimble showing micropores, X400.

Table 2. Typical EDX atom % content results for YSZ thimbles, type A and type B

Elements	Atom % content					
	Grain-interior spot		Glassy phase spot		Area (including grain-interior and grain boundary) analysis	
	A	*B*	*A*	*B*	*A*	*B*
Zr	28.0	27.9	3.5	–	27.3	27
Y	6.4	6.5	2.1	–	5.6	6.3
Al	–	–	11.5	–	0.7	–
Ca	–	–	6.8	–	1.2	–
Si	–	–	14.0	–	–	–
O	65.6	65.6	62.1	–	65.2	66.7

analysis of the grain-interior, glassy phase at the grain boundary and an area analysis that includes grain-interior and grain boundaries of the YSZ samples were performed and the results are shown in Table 2. It can be seen that there was co-segregation of aluminium, calcium and silicon in the glassy phase at the grain boundary of type A YSZ thimbles. Although the silicon atom% content is very high (14%) in the glassy phase, it was not detected in the grain-interior and in the area EDX analysis.

5. Thermodynamic analysis of results

To aid thermodynamic calculation of cell potentials, some values for terms in Equation 22 over a range of temperature have been calculated and listed in Table 3. In calculating $(2.303RT/2F)\log(f_{H_2}/a_{H_2O})$, it is reasonable to set $(\gamma_{H_2}/\gamma^{\circ}_{H_2})(1/a_{H_2O}) \approx 1$ in dilute solutions and at low hydrogen concentrations. K_H and K°_H can be found from the literature [19].

The first YSZ $(Ag|O_2)$ pH sensor was made using a type A YSZ thimble. This sensor can give reliable and repeatable potential data when the temperature is not lower than 150 °C. Our experimental data using this sensor for the YSZ $(Ag|O_2)|H_2(Pt)$ cell potential in three different Lithium ion concentration solutions are listed in Table 4 together with the calculated data using the modified thermodynamic approach. It can be seen that the cell potentials are similar in the three solutions and that general agreement between the experimental data and the calculated data exists. The published experimental data obtained by Danielson et al. [12] for the YSZ $(Ag|O_2)|H_2(Pt)$ cell potential (which have been averaged) and their calculated data are listed in Table 5 and shown in Figure 4. Our test results, which are averaged, and calculated data using the modified calculation are also listed in Table 5 and shown in Figure 4 for comparison. Good agreement between the two sets of experimental data and the calculated data using the new calculation can be seen. Danielson's calculation has good agreement with the experimental data at 200 °C and 250 °C. At lower and higher temperatures, their calculation has larger differences with the experimental data because they did not make a correction for the oxygen partial pressure with temperature. Although not shown in Figure 4, the modified calculation data also deviates from Danielson's at temperatures above 350 °C and is likely to be a better approximation of the actual

Table 3. Calculated values of terms in Equation 22 as a function of temperature

Temp. /°C	$-\frac{2\mu^{\circ}_{H_2O} - \mu^{\circ}_{O_2} - 2\mu^{\circ}_{H_2}}{4F}$ /mV	$\frac{2.303\,RT}{2F}\log\left(\frac{f_{H_2}}{a_{H_2O}}\right)$ $(f^{\circ}_{H_2} \approx 1)$/mV	$\frac{2.303\,RT}{2F}\log\left(\frac{f_{H_2}}{a_{H_2O}}\right)$ $(f^{\circ}_{H_2} \approx 0.1)$/mV
100	1167	−2	−39
125	1147	−5	−44
150	1127	−8	−50
175	1107	−13	−56
200	1088	−17	−64
225	1069	−22	−71
250	1050	−28	−80
300	1012	−42	−99
350	975	−58	−120

Table 4. Experimental data for $\Delta E = E_{YSZ(Ag/O_2)} - E_{Pt/H_2}$ and calculated data using the modified approach

Temp. /°C	Experimental data /mV			Calculated data from Eqation 28 /mV
	0.01 M H_3BO_3 + 0.0001 M LiOH	0.01 M H_3BO_3 + 0.001 M LiOH	0.01 M H_3BO_3 + 0.01 M LiOH	
150	1084	1089	1090	1102
200	1052	1057	1059	1061
250	1008	1009	1009	1010
300	960	957	953	959

Table 5. YSZ ($Ag|O_2$)$|H_2$ (Pt) cell potential experimental data in comparison with calculated data by Danielson [12] and using the modified approach

Temp. /°C	Calculated data by Danielson [12] /mV	Calculated data from Equation 28 modified method /mV	ΔE experimental data (averaged) from [12] /mV	ΔE experimental data (averaged) from Table 3 /mV
100	1158	1134	1113	–
150	1112	1102	1096	1088
200	1062	1061	1065	1056
250	1009	1010	1017	1009
300	951	959	966	957
350	895*	905	–	–

* Extrapolated data.

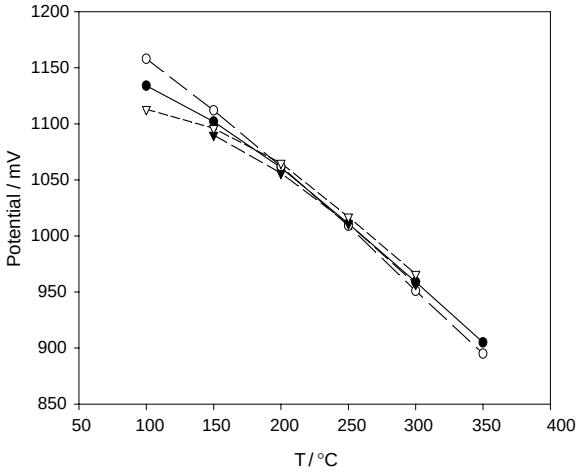

Fig. 4. Comparison of YSZ ($Ag|O_2$) vs H_2(Pt) averaged cell potential data in various alkali/boric acid solutions compared with calculated data by two methods. Key: (●) new calculation; (○) calculated by Danielson [12]; (▼) experimental data; (▽) experimental data by Danielson [12].

behaviour. The experimental data for the YSZ ($Ag|O_2$)$|H_2$(Pt) cell potentials obtained by Danielson et al. are slightly higher than our data and this is probably due to different oxygen partial pressures inside the electrode tubes. We placed pure silver powder into the YSZ tube, while Danielson et al. coated the inside surface of the YSZ tube using silver paste which was dried by heating. The heating process may have produced some Ag_2O which decomposed during high temperature tests. Our test results, Danielson's test results, and the modified calculated data indicate that the YSZ ($Ag|O_2$) pH sensor is a primary pH sensor.

Later a type B YSZ thimble which was verified by electrochemical impedance spectroscopy (EIS) to have an impedance lower than the type A YSZ thimbles, was used to prepare a YSZ ($Ag|O_2$) pH sensor. The sensor was expected to work at lower temperatures and it was tested successfully over the temperature range 100–300 °C in 0.001 M KOH + 0.009 M KCl solution. Tests at 185 °C and 170 °C were performed to determine a more accurate temperature limit for the agreement between the experimental results and the new thermodynamic calculation. Below the temperature limit, the oxygen partial pressure is better calculated using $\Delta G^{\circ}_{\text{metal/metal oxide}}$, above the temperature limit, the oxygen partial pressure is better calculated using the ideal gas equation because of the complete decomposition of the silver oxide. Measured YSZ ($Ag|O_2$)$|H_2$(Pt) cell potentials in comparison with calculated cell potentials by the two methods are shown in Table 6. From Table 6 it can be seen that when the temperature is lower than 170 °C, cell potentials calculated using $\Delta G^{\circ}_{\text{metal/metal oxide}}$ to determine P_{O_2} have better agreement with experimental results, because below this temperature oxygen starts to react with silver powder to produce silver oxide. It is the silver/silver oxide reaction equilibrium that

Table 6. YSZ ($Ag|O_2$)$|H_2$ (Pt) cell potentials measured in 0.001 M KOH + 0.009 M KCl in comparison with calculated cell potentials from thermodynamic approach

Temp. /°C	Cell potentials measured /mV	Cell potentials calculated using $\Delta G^{\circ}_{\text{Metal/Metal Oxide}}$ calculating P_{O_2}/mV	Cell potentials calculated using ideal gas Equation calculating P_{O_2}/mV
100	1133	1134	1154
125	1117	1118	1131
200	1099	1102	1107
170	1082	1090	1090
185	1067	1075	1071
200	1062	1116	1061
225	1036	1049	1035
250	1012	1030	1010
275	988	1037	985
300	960	990	959

Table 7. Comparison of YSZ (Hg|HgO)|H_2 (Pt) cell potential experimental data from [4] with calculated data from Equation 28 and Equation 5

Temp. /°C	Calculated data from Equation 28 modified method /mV	Calculated data from Equation 5 Macdonald's method /mV	ΔE experimental data in 0.01 M $B(OH)_3$ + 0.01 M KOH /mV	ΔE experimental data in 0.01 M KOH /mV
125	906	908	891	910
150	894	899	884	887
175	883	889	874	876
200	871	878	867	866
225	859	866	856	855
250	848	853	845	843
300	824	823	826	820
350	801	788*	–	–

* Extrapolated data.

determines the oxygen partial pressure. When the temperature is higher than 170 °C, cell potentials calculated using the ideal gas equation for P_{O_2} agree with experimental results better, because when silver oxide decomposes to silver and oxygen, there is negligible silver oxide.

The thermodynamic approach is also applicable to other internal element YSZ pH sensors. The YSZ (Hg|HgO)|H_2(Pt) cell potentials in 0.01 M $B(OH)_3$ + 0.01 M KOH and in 0.01 M KOH solution over a range of temperature were published by D.D. Macdonald et al. [4]. The experimental data along with the calculated data from Equation 28 (our method) and Equation 5 (Macdonald's method) are listed in Table 7 and are also shown in Figure 5 for comparison. Good agreement can be found between the experimental data and the calculated data using the two methods. In fact, the $-((2\mu^\circ_{H_2O} - \mu^\circ_{O_2} - 2\mu^\circ_{H_2})/4F) + (RT/4F)\ln(P_{O_2})$ term has good agreement with the $E^\circ_{Hg/HgO}$ term listed by Naumov et al. [20] which is related to the change in standard chemical potential for the reaction:

$$HgO + 2\,H^+ + 2\,e^- = Hg + H_2O \qquad (29)$$

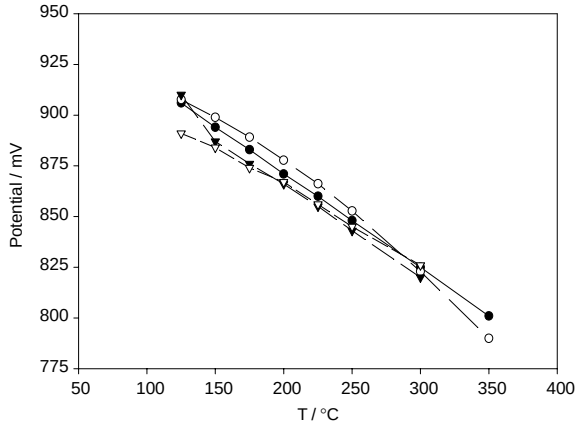

Fig. 5. Comparison of YSZ (Hg|HgO) vs H_2(Pt) cell potential data with calculated data by two methods. Key: (●) new calculation; (○) calculated by Macdonald [4]; (▼) experimental data in 0.1 M KOH [4]; (▽) experimental data in 0.1 M $B(OH)_3$ + 0.01 M KOH [4].

When the oxygen partial pressure is equal to the equilibrium partial pressure for the metal/metal oxide reaction inside the YSZ tube, our calculation and Macdonald's calculation should give the same values. The small variations between the two sets of calculated data arise from the different sources used for the basic thermodynamic parameters.

For the YSZ (Cu|Cu_2O)|H_2(Pt) cell, when there is excess oxygen in the YSZ tube, two reactions may occur:

$$2\,Cu + O_2 = 2\,Cu_2O \qquad (30)$$

$$2\,Cu_2O + O_2 = 4\,CuO \qquad (31)$$

In this case the equilibrium oxygen partial pressure can not be calculated from Equation 9. If the oxygen content in the YSZ tube is just enough to induce the reaction described in Equation 30 only, then the equilibrium oxygen partial pressure can be calculated from Equation 9. This means that to use Cu|Cu_2O as an internal element, the oxygen content has to be controlled so that the equilibrium condition relates to reaction 30. The first YSZ (Cu|Cu_2O)|H_2(Pt) cell potentials were published by Niedrach [2, 3] and have good agreement with the calculated potential from Equation 28 using the oxygen partial pressure for Reaction 30. From Equation 9, the Cu|Cu_2O cell at 285 °C yields: $(RT/4F)\ln(P_{O_2}) \approx -650$ mV, $(2.303\,RT/2F)\log(f_{H_2}/a_{H_2O}) \approx -92$ mV ($f^\circ_{H_2} \approx 0.1$) and $-(2\mu^\circ_{H_2O} - \mu^\circ_{O_2} - 2\mu^\circ_{H_2})/4F \approx 1023$ mV then the YSZ(Cu|Cu_2O)|H_2(Pt) cell potential at 285 °C is: $\Delta E = E_Y - E_{Pt/H_2} \approx 1023 - 650 - 92 = 281$ mV. The ΔE values acquired from experiments by Niedrach were: 274, 272 and 280 mV [3].

6. Conclusions

A modified thermodynamic approach to the calculation of the YSZ pH sensor potential related to the molar Gibbs free energies (chemical potentials) of reactants and products has been developed that can support the published experimental data including that for YSZ (Ag|O_2)|H_2 (Pt), YSZ (Hg|HgO)|H_2 (Pt) and YSZ (Cu|Cu_2O)|H_2 (Pt) cells over a wide range of

temperature. The modified thermodynamic calculation and our experimental results from refreshed autoclave tests confirm that the YSZ ($Ag|O_2$) pH sensor is a primary pH electrode. This modified approach can provide a calculation of the YSZ pH sensor and the H_2 (Pt) electrode half-cell potentials.

Acknowledgements

The authors gratefully acknowledge the advice of Professor R.D. Armstrong, Professor A.K. Covington, Dr J. Congleton and Dr M. Todd.

References

1. D.D. Macdonald and L.B. Kriksunov, *Electrochim. Acta* **47** (2001) 775.
2. L.W. Niedrach, *J. Electrochem. Soc.* **127** (1980) 2122.
3. L.W. Niedrach and W.H. Stoddard, *J. Electrochem. Soc.* **131** (1984) 1017.
4. D.D. Macdonald, S. Hettiarachchi and S.J. Lenhart, *J. Solut. Chem.* **17** (1988) 719.
5. D.D. Macdonald, S. Hettiarachchi, S. Herking, K. Makela, R. Emerson and M. Ben-Hai, *J. Solut. Chem.* **21** (1992) 849.
6. T. Tsuruta and D.D. Macdonald, *J. Electrochem. Soc.* **128** (1981) 1199.
7. T. Tsuruta and D.D. Macdonald, *J. Electrochem. Soc.* **129** (1982) 1221.
8. S. Hettiarachchi and D.D. Macdonald, *J. Electrochem. Soc.* **131** (1984) 2206.
9. S. Hettiarachchi and D.D. Macdonald, *J. Electrochem. Soc.* **134** (1987) 1307.
10. S. Hettiarachchi, K. Makela, H. Song and D.D. Macdonald, *J. Electrochem. Soc.* **139** (1992) 13.
11. S.N. Lvov and D.D. Macdonald, *J. Electroanal. Chem.* **403** (1996) 25.
12. M.J. Danielson, O.H. Koski and J. Myers, *J. Electrochem. Soc.* **132** (1985) 296.
13. K. Ding and W.E. Seytried, *Science* **272** (1996) 1634.
14. K. Eklund, S.N. Lvov and D.D. Macdonald, *J. Electroanal. Chem.* **437** (1997) 99.
15. S.N. Lvov, H. Gao and D.D. Macdonald, *J. Electroanal. Chem.* **443** (1998) 186.
16. J.D. Gilchrist, 'Extraction Metallurgy', 3rd edn (Pergamon Press, 1989).
17. E.H. Oelkers, H.C. Helgeson, L.S. Everett, A.S. Dimitri, J.W. Johnson and A.P. Vitalii, *J. Phys. Chem. Ref. Data* **24** (1995) 1401.
18. J.O'M. Bockris and S.U.M. Khan, 'Surface Electrochemistry' (Plenum, NewYork, 1993).
19. D.M. Himmelblau, *J. Chem. Eng. Data* **5** (1960) 10.
20. G.B. Naumov, B.N. Ryzhenko and I.L. Khodakovsky, 'Handbook of Thermodynamic Data', USGS-WRD-74-001 (1974).